To appear in the *Journal of Geophysical Research*, 2001.

Near-Sun and near-Earth manifestations of solar eruptions

N. Gopalswamy,[1,2] A. Lara,[1,3] M. L. Kaiser,[4] and J.-L. Bougeret[5]

Abstract

We compare the near-Sun and near-Earth manifestations of solar eruptions that occurred during November 1994 to June 1998. We compared white-light coronal mass ejections, metric type II radio bursts, and extreme ultraviolet wave transients (near the Sun) with interplanetary (IP) signatures such as decameter-hectometric type II bursts, kilometric type II bursts, IP ejecta, and IP shocks. We did a two-way correlation study to (1) look for counterparts of metric type II bursts that occurred close to the central meridian and (2) look for solar counterparts of IP shocks and IP ejecta. We used data from Wind and Solar and Heliospheric Observatory missions along with metric radio burst data from ground-based solar observatories. Analysis shows that (1) most (93%) of the metric type II bursts did not have IP signatures, (2) most (80%) of the IP events (IP ejecta and shocks) did not have metric counterparts, and (3) a significant fraction (26%) of IP shocks were detected in situ without drivers. In all these cases the drivers (the coronal mass ejections) were ejected transverse to the Sun-Earth line, suggesting that the shocks have a much larger extent than the drivers. Shocks originating from both limbs of the Sun arrived at Earth, contradicting earlier claims that shocks from the west limb do not reach Earth. These shocks also had good type II radio burst association. We provide an explanation for the observed relation between metric, decameter-hectometric, and kilometric type II bursts based on the fast mode magnetosonic speed profile in the solar atmosphere.

1. Introduction

Solar eruptions are violent activities that dump huge amounts of energy into the inner heliosphere in the form of coronal mass ejections (CMEs), flares, prominence eruptions, energetic particles, and shock waves. Of these, shock waves are of particular interest because they produce radio emission at various distances from the Sun starting from the inner corona to the orbit of Earth and beyond. Shocks also accelerate solar energetic particles and produce storm sudden commencement at Earth. Close to Earth, shocks can be detected in situ by spacecraft in the solar wind. The shocks at 1 AU are almost always associated with fast CMEs [*Sheeley et al.*, 1985; *Cane et al.*, 1987]. However, the association between shocks and CMEs is not so clear near the Sun. Although CME events have been well studied in the near-Sun and near-Earth domains, very few works deal with the relation between the two domains [*Gopalswamy et al.*,1998; *Reiner and Kaiser*, 1999]. In this paper we explore the relation between what we know in these two domains using a set of well-observed solar eruptive events.

One of the current issues in the study of solar eruptions is that there is minimal overlap between coronal and interplanetary (IP) shock populations [*Gopalswamy et al.*,1998 ; Cliver et al., 1999]. Even though both populations are of solar origin, the coronal population does not seem to result in the IP population. To understand the relation between coronal and IP shocks, we need to consider events from all positions in the Sun-Earth connected space: type II bursts, CMEs, IP ejecta, and IP shocks detected in situ. Fortunately, we have a large array of space- and ground-based instruments which gather data on all these phenomena so we can better relate the near-Sun and near-Earth manifestations of solar eruptions. In a previous attempt, *Gopalswamy et al.* [1998] (hereinafter referred to as paper 1) started with metric type II bursts and looked for (1) their continuity in the decameter-hectometric (DH) window newly opened by the Wind/WAVES experiment [*Bougeret et al.*, 1995], and (2) IP shocks detected in situ. They also performed a reverse correlation by searching for metric type II bursts 1-5 days prior to the detection of IP shocks. Both searches ended in a negative result, on the basis of which it was concluded that the shocks responsible for metric type II bursts and the IP shocks are of independent origin. No radio burst occurred in the outer corona (the DH spectral domain) during the study period considered in paper 1. Since then, a large number of type II bursts have been observed in the DH domain [*Gopalswamy et al.*, 1999a; 2000b; *Kaiser et al.*, 1998; *Reiner and Kaiser*, 1999] and IP shocks have been detected *in situ*, so we can revisit the issue with a much larger data set.

Since the launch of Wind in November 1994, the WAVES experiment detected 70 events until June 1998 which represent shock waves and/or mass motions far away from the Sun. This data set represents an important source to identify disturbances leaving the Sun (which are important for space weather applications). Twenty-seven of these 70 events produced radio signatures in the previously unexplored frequency regime (1-14 MHz) which serve as a bridge to understand the evolution of metric radio phenomena as they propagate into the IP medium. There were 51 kilometric type II bursts, due to shocks propagating far into the IP medium, close to Earth. Most of the WAVES events were type II bursts, and in a very small number of cases type IV bursts were also observed. We make use of these radio bursts in probing

the relationship between near-Sun and near-Earth manifestations of solar eruptions.

2. Data Selection

Our study period starts from the launch of Wind spacecraft in November 1994 and ends in the middle of June 1998 when the Solar and Heliospheric Observatory (SOHO) became temporarily disabled. Combining SOHO and Wind data has proved to be a powerful means of studying the origin and interplanetary propagation of solar disturbances. The data set used in this study consists of the following four major components:

The first is metric, DH, and kilometric type II radio bursts. We collected all the metric type II bursts reported in the Solar Geophysical Data for our study period. These bursts were observed by ground-based radio telescopes at various observatories from around the world. There were in all 137 type II bursts. The ground-based instruments cover a frequency range of ~18-2000 MHz. The DH and kilometric type II bursts were recorded by the WAVES experiment on board the Wind spacecraft. The WAVES experiment consists of two receivers, RAD1 (20-1040 kHz) and RAD2 (1.075-13.825 MHz), that detect kilometric and DH radio emissions, respectively. The RAD2 spectral domain is just below the metric domain and hence bridges the long-existing gap between the kilometric and metric domains.

The second component is white-light CMEs. SOHO mission's Large-Angle and Spectrometric Coronagraph (LASCO) [*Brueckner et al.*, 1995] detects CMEs in the range 1.1-30 R_s using its three telescopes, named C1 (1.1-3 R_s), C2 (1.5-6 R_s), and C3 (3.5-30 R_s). The LASCO began recording CMEs in January 1996 and has accumulated more than 800 CMEs until June 1998. Out of these, 638 CMEs had good measurements of properties such as speed, position angle (PA), and width [*St. Cyr et al.*, 2000]. The CMEs constitute one of the primary near-Sun manifestations of solar eruptions, others being flares, prominence eruptions, and metric type II bursts.

The third component is IP events. On the basis of data from the Wind spacecraft's Solar Wind Experiment (SWE) [*Ogilvie et al.*, 1995] and Magnetic Fields Investigation (MFI) [*Lepping et al.*, 1995], a catalog of IP events is maintained by the Science Planning and Operations Facility (SPOF) of the International Solar-Terrestrial Physics (ISTP) group at the NASA Goddard Space Flight Center [*Acuña et al.*, 1995]. The SPOF catalog consists of all significant IP signatures. We searched for IP events of solar origin such as magnetic clouds (MCs), other ejecta (E), and IP shocks. The main difference between MCs and Es is that the former have a flux-rope magnetic field structure [e.g., *Burlaga et al.*, 1981]. In the present paper, IP ejecta refers to all ejecta, irrespective of their magnetic structure. We identified 49 IP events during the study period, 46 of which had IP shocks preceding them. There were 37 IP ejecta (29 MCs and 8 Es) and 13 isolated IP shocks with no associated IP ejecta. IP shocks preceded 27 MCs and all but one of the Es. This represents a large population of IP shocks compared with only three in the study period of paper 1.

The fourth component is flares. We used temporal, positional, and brightness information of flares associated with the radio bursts from the Solar Geophysical Data. We also used EUV images from SOHO's extreme ultraviolet imaging telescope (EIT) [*Delaboudiniere et al.*, 1995] to verify the flare location and transient activity near the solar surface.

The EIT data are also used to discriminate between frontside and backside CME events observed by LASCO. A typical EIT event consists of one or more of the following signatures: an EIT wave, an EUV dimming, and posteruption arcade formation [*Thompson et al.*, 1998; *Gopalswamy and Thompson*, 2000, and references therein]. The images used in this study have a cadence of ∼15 min obtained in the 195-Å band, which corresponds to a coronal temperature of ∼1.5 MK.

3. Analysis and Results

Our analysis consists of the following three parts: (1) We start from metric type II bursts that occur on the solar disk and search for counterparts in the IP medium such as DH type II bursts, kilometric type II bursts, and IP ejecta observed in situ. (2) We start from the cataloged IP events and search for metric, DH, and kilometric type II bursts. (3) We start from DH type II bursts and search for metric type II bursts (near the Sun) and kilometric type II bursts and in situ IP events. For steps 2 and 3 we relaxed the constraint that metric type II bursts must be disk events. In this analysis we assume that the maximum time taken by a solar disturbance to reach 1 AU to be ∼5 days and we assume the minimum time to be ∼1 day.

3.1. Metric Type II Bursts, CMEs, and IP Events

Out of the 137 metric type II bursts, we selected those events that occurred close to the Sun center (central meridian distance $< 60°$) because these are expected to be associated with Earth directed disturbances. Coronal shocks responsible for the metric type II bursts on the disk are likely to be detected as the IP shocks if the two populations are the same. The simplest thing to do is to see whether IP shocks were detected at 1 AU 1-5 days after the metric type II burst. We give primary importance to in situ shocks because, radio emission in the IP medium has to satisfy other constraints such as electron acceleration by the shocks, production of plasma waves by the energetic electrons, and the conversion of plasma waves into electromagnetic radiation detected as type II bursts.

We found 44 metric type II bursts that can be regarded as disk events (see Table 1). In columns 2, 3 and 4, we have listed the date, starting frequency (f_s), in megahertz, and the onset time, respectively, for each of the type II bursts. In columns 5-8, we have listed the starting and ending times, heliographic location, NOAA active region number, and the X-ray/optical importance of the associated flare. When there is no optical flare reported, we have given just the X-ray importance. If a LASCO CME is associated with a metric type II burst, we have listed the CME speed in column 9, with an additional letter H if it was a halo CME. Halo CMEs first detected by *Howard et al.* [1982] appear to surround the occulting disk because they propagate toward or away from Earth. CMEs with widths exceeding ∼120° are listed as halo CMEs. If there was no reported CME, we have marked N, for no in column 9, while ND (no data) and DG (data gap) denote lack of data. In column 10, we have stated whether there was an associated DH type II burst (Y for yes; N for no); a question mark is added for those cases in which the association is fortuitous. Month/day in column 11 identifies the kilometric type II burst within the expected time window (1-5 days) following the metric type II burst, while N denotes that there was no kilometric type II burst. In column 12, information on the associated IP ejecta is listed:

N means no IP ejecta; MC means magnetic cloud; E means ejecta without flux rope structure; and S means IP shock; when an IP event was found within 1-5 days after the metric type II burst, we have listed the month and day of the event. For example, MC/S 5/15 means a magnetic cloud with IP shock was detected in situ on May 15, 1997, following the metric type II burst of May 12, 1997. Entries with a question mark do not have an actual association with the metric type II bursts (see later).

3.2. Metric Type II Bursts and Flares

All the type II bursts were associated with active region flares, except for the May 19, 1998, event, which was a purely filament eruption event but had a weak GOES flare. The GOES flare listed in the Solar Geophysical Data was from the southwest quadrant, while the filament eruption was from the northwest quadrant. The filament eruption was associated with a CME. This also is the only event in which the flare started after the type II onset. In all other cases the type II burst onset followed the GOES flare onset by at least a few minutes (compare columns 4 and 5 in Table 1). In all the cases the flares were from identified active regions (see Table 1). We can also see that the metric type II bursts originated from 26 different active regions, suggesting that some active regions are prolific producers of metric type II bursts. The X-ray importance of flares ranged from B to X, while the optical importance also had the full range from subflares to 3B. Thus the intimate relationship between flares and type II bursts is confirmed, although the nature of the relationship is still not clear.

3.3. Metric Type II Bursts and CMEs

The SOHO mission had data coverage only for 32 metric type II bursts listed in Table 1. Out of the 32 metric type II bursts, 21 (66%) were associated with CMEs detected by SOHO coronagraphs. Since these are disk events, it is somewhat difficult to detect the associated CMEs by coronagraphs. However, most of these metric type II bursts were associated with EIT waves. *Cliver et al.* [1999] concluded that almost all the metric type II bursts during the Solwind period were indeed associated with CMEs, supporting earlier conclusions by *Munro et al.*, [1979] and *Gosling et al.*, [1976]. Details of the association between white-light CMEs and metric type II bursts during our study period is reported elsewhere (E. W. Cliver et al., manuscript in preparation, 2000).

The close association between metric type II bursts and white-light CMEs is taken to suggest that CMEs are fast enough to drive coronal shocks. In Figure 1 we have shown the speed distribution for three populations of LASCO CMEs: all CMEs with measurable speeds (Figure 1a), CMEs associated with metric type II bursts (Figure 1b), and CMEs associated with metric type II bursts that occurred close to the limb (Hα flare longitudes $> 60°$) (Figure 1c). There is virtually no difference between the populations in Figures 1b and 1c, while they substantially differ from the population in Figure 1a. This definitely suggests that the CMEs with type II bursts are slightly faster as a class. In the past, CMEs with type II bursts were found to have speeds exceeding 400-550 km s^{-1} [see, e.g., *Gosling et al.*, 1976]. The present data (Figure 1) show that a large number (13/26 or 50%) of CMEs with type II bursts have speeds $<$500 km s^{-1}. Moreover, the speeds of CMEs with type II bursts had a lower cutoff of $\sim$250

km s^{-1}, which is considerably lower than 400 km s^{-1} obtained by *Gosling et al.* [1976]. Our low-speed cutoff is accurate because we have considered limb events separately for which the CME speed measurement is free from projection effects.

Most of the type II bursts without CMEs, however, were associated with EIT wave transients. It is now known that almost all of the metric type II bursts are associated with EIT waves [*Klassen et al.*, 2000]. At least half of these EIT waves associated with the CME-less type II bursts were "brow waves," which may be the shock waves responsible for type II bursts [Gopalswamy et al., 2000c; *Gopalswamy and Thompson*, 2000]. The brows are typically located to the equatorial side of the associated active regions. Figure 2 shows an example of the brow wave that occurred on November 3, 1997, at 0912 UT (event 32 in Table 1). Clearly, the outermost structure from the eruptive region is a brow wave. We see that the brow wave is located outside the active region (toward the equator) at the time of the metric type II burst.

We also note that the metric type II bursts with no associated CMEs had also no associated DH or kilometric type II bursts. (There was a kilometric type II burst for event 39 in Table 1, but the association is fortuitous because the kilometric type II was actually associated with event 40.)

3.4. Metric Type II Bursts and IP Events

The last three columns in Table 1 show all the possible associations of metric type II bursts with IP signatures: DH type II bursts, kilometric type II bursts, and *in situ* IP events. The DH type II bursts are not exactly interplanetary, but outer coronal; they serve as the earliest indication that the disturbance from the solar eruption is moving beyond $\sim$2 R_s from the Sun. We now discuss the association of metric type II bursts with each one of these signatures.

3.4.1. DH type II bursts. We note that only eight out of the 44 metric type II bursts (18%) were associated with DH type II bursts. The last two metric type II bursts (events 43 and 44 in Table 1) had DH type II bursts in the appropriate time window, but they are known to be associated with other eruptions that did not produce metric type II bursts [*Gopalswamy et al.*, 2000b]. Even in those cases with DH and metric type II association, the relationship can be quite complex [*Kaiser et al.*, 1998; *Gopalswamy et al.*, 1999a; *Reiner and Kaiser*, 1999; *Reiner et al.*, this issue].

3.4.2. Kilometric type II bursts. There were 11 kilometric type II bursts in the appropriate time windows following the metric type II bursts (Table 1, column 11). However, the number of kilometric type II bursts that occurred during the study period is much larger (51). A vast majority of them did not have associated metric type II bursts. Therefore, at least in some of the 11 cases, the association may be fortuitous. Since we have not completed identifying the solar sources of all the 51 kilometric type II bursts, we cannot say how many of the 11 kilometric type II bursts within the expected time windows of metric type II bursts are fortuitous. What we can definitely say is that the upper limit for the fraction of metric type II bursts associated with kilometric type II bursts is $\sim$25%. This is much smaller than the 70% association found between kilometric type II bursts and metric type II bursts by *Cane and Stone* [1984]. We shall discuss this discrepancy in a later section.

3.5. Metric Type II Bursts and IP Events

In Table 1 we see that there were only eight different IP ejecta within the anticipated time windows of nine different metric type II bursts. This is a small overlap considering the large number of IP ejecta (37) and metric type II bursts (44) detected during the study period. This in itself is a poor association. When we made careful matching of the metric and the in situ events, we found that about half of the associations were fortuitous. We discuss these events individually so we can assess the actual extent of positive association between metric and IP events.

3.5.1. February 8, 1995, MC. This MC was in the appropriate time window of the February 4, 1995, metric type II burst. There were a few disappearing solar filaments (DSFs) associated with this MC. Since DSFs are usually associated with CMEs, it is difficult to unambiguously associate the metric type II burst with the MC. The SOHO observations began only in January 1996, so no CME data are available for this event.

3.5.2. October 10, 1997, MC. This MC occurred 33 hours after the metric type II burst on October 9 at 1158 UT. Near the Sun the metric type II burst was associated with a CME which had a speed of only 233 km s^{-1}. It is highly unlikely that such a slow CME was able to reach 1 AU in 33 hours. The October 10 MC was indeed associated with the October 6, 1997, halo CME from 54°S, 46°E with no associated metric type II burst [*Gopalswamy et al.*, 2000a].

3.5.3. November 7, 1997, MC. This MC has five potential matches from the metric domain (three on November 3, 1997, and two on November 4, 1997: events 31-35 in Table 1). At least three of these metric type II bursts were associated with white-light CMEs, and two of them had associated DH type II bursts (the November 3, 1997, event at 0437 UT and the November 4, 1997, event at 0558 UT). Unless the November 7 MC is due to a combination of all these CMEs and type II bursts, the November 4 halo CME seems to be the likely solar source of this MC [*Gopalswamy et al.*, 2000a]. Then the correct metric type II burst to be associated with the MC is the one on November 4 at 0558 UT (event 34 in Table 1).

3.5.4. May 2, 1998, MC. This is one of the few MCs that did not have an associated IP shock. There were two possible metric type II bursts on April 29, 1998 (events 39 and 40 in Table 1), in the expected time window of this MC. The first one, at 0831 UT, did not have an associated CME, while the second one, at 1622 UT, was associated with a halo CME. The MC seems to have originated from this halo CME, so the appropriate metric type II is the one on April 29 at 1622 UT. The May 4, 1998, IP ejecta (E) is also within the time window of these metric type II bursts but is known to be associated with the halo CME of May 2, 1998, which had no associated metric type II burst [*Gopalswamy et al.*, 2000a].

3.5.5. June 24, 1998, MC. This was another MC without a shock at 1 AU and was in the time window of the metric type II events 43 and 44. The solar source seems to be the interconnecting loop CME of June 21, 1998, with no metric type II burst.

Thus only four out of the 44 type II bursts (9%) seem to have a positive association with IP ejecta. These are the metric type II bursts on April 7, May 12, and November 4 (at 0558 UT) in 1997 and on April 29 (at 1622 UT) in 1998. All the four events consisted of large-scale halo CME events. Moreover, all the

events except the one on April 29, 1998, had DH and kilometric type II events. These results suggest that the metric type II bursts are poor indicators of IP signatures at least for the 3-year period (November 1994 to June 1998) considered in this work, consistent with our previous conclusions in paper 1. From Table 1 we also see that these four "end-to-end" events were associated with only weak flares: Three of them were C-class flares, while only one was M-class. On the other hand, we see many metric type II bursts associated with M-class flares but not followed by IP ejecta. The soft X-ray flare durations of the end-to-end events ranged only from 10 to 53 min. The optical flares associated with the end-to-end events seem to have a higher importance: 3N, 2B, and 3B for the April 7, 1997, November 4, 1997, and April 29, 1998 events, respectively; no classification was reported for the May 12, 1997, event.

3.6. IP Events and All Metric Type II Bursts

In the previous sections we considered only disk type II bursts, which constitute only about a third of all metric type II bursts in the study period. We now perform a reverse search for possible metric type II associations within 5 days prior to the IP events. We have listed all the IP events detected by Wind in Table 2. In columns 2 and 3 we list the date and onset time of each IP event, with its type (MC, E, and S) given in column 3. The speed of the IP event at 1 AU is given in column 4. In columns 5-7 the possible associations with metric, DH, and kilometric type II bursts are noted (N for no, Y for yes). If there was a metric type II burst within the appropriate time window, we have indicated the month and day of the burst in column 5. If the association is fortuitous, we have added an asterisk in column 5 and included a discussion in the text as to why we think the association is not positive. In column 8, we have listed the solar source of the IP event. We specifically looked for CMEs. When no CME observations were made, we searched for DSFs. Halo CMEs are marked as HCME. The month, day, and UT times of the solar source are also given in column 8. In column 9 we have listed the latitude and longitude of the location of eruption. In the last column we have listed the CME speed if available; DG and ND denote data gap and no data, respectively. A question mark in columns 8 and 9 indicates the associations are less confident.

Note that 46 out of 49 IP events (94%) had shocks, so it is appropriate to look for metric type II bursts if these shocks were a continuation of coronal shocks. In looking for metric type II bursts associated with IP shocks, we relaxed the criterion that the type II bursts should be within a central meridian distance of 60°. Thus we are considering all the 137 metric type II bursts and 49 IP events during our study period. Note that the IP events include 12 isolated shock events without obvious drivers behind them. These shocks appear isolated or "driverless" because they are produced by limb CMEs; the spacecraft intercepts only a flank of the CME-driven shocks.

When we searched for metric type II bursts 1-5 days before the onset of the IP events, we found only six new associations, in addition to the four associations found in Table 1. All of these new associations between metric type II bursts and IP events are for isolated shock cases. There were a few additional cases in which the association between metric type II bursts and IP events seems to be chance coincidence. These cases are discussed below.

3.6.1. September 21, 1997, MC. The only metric type II burst within the appro-

priate time window of this MC is the one on September 17, 1997, at 1144 UT, associated with an M flare at 21°N, 82°W and a LASCO CME at the appropriate position angle. It is unlikely that such a limb CME would be detected as an ejecta *in situ* at 1 AU. Instead, the MC seems to be due to a halo CME on September 17, 1997, at 2028 UT from 30°N, 10°W (see Table 2).

3.6.2. October 1, 1997 MC. Three metric type II bursts were within the time window of this MC: the September 26, 1997, burst at 1454 UT (slightly more than 5 days before the MC; it originated from behind the east limb, but no obvious white-light CME was detected), the September 28, 1997, burst at 0803 UT (behind the east limb; CME was at PA ∼70°), and the September 28, 1997, burst at 1419 UT (behind the east limb; CME was at PA ∼90°). As we argued before, limb and backside events are unlikely to be detected as ejecta near Earth. The MC in question was most likely associated with the 0108 UT halo CME and DSF on September 28, 1997, from 22°N, 5°E.

3.6.3. October 10 1997, MC. Two metric type II bursts could be found in the appropriate time window of this MC. The first one was on October 7, 1997, at 1249 UT from behind the west limb and was associated with a fast (speed, 1300 km s^{-1}) CME at PA ∼240°. This limb CME could not have caused the October 10 MC. The second one was on October 9, 1997, at 1158 UT associated with a slow (speed, 233 km s^{-1}) CME at PA ∼78°; the location of the eruption seems to be 24°N, 36°E. It is unlikely that such a slow eruption reaches 1 AU in 23 hours. The MC was in fact associated with the October 6, 1997, halo CME at 1528 UT.

3.6.4. January 24, 1998, S. The January 19, 1998, metric type II burst at 0658 UT is in the appropriate time window of this shock. However, the metric type II burst was associated with a CME at 0733 UT (PA ∼290°; speed, 358 km s^{-1}) originating from behind the northwest limb. The shock is more likely due to the halo CME with DSF originating from the southern polar crown region (57°S, 19°E) on January 21, 1998, at 0637 UT. The IP ejecta from this halo event is likely to have missed the spacecraft because of its deeply southern location on the solar disk.

3.6.5. January 28, 1998, S. Two metric type II bursts were in the right time window of this shock: The first one was on January 25, 1998, at 2135 UT from 22°N, 53°E, associated with a fast (speed ∼773 km s^{-1}) CME at PA ∼80°. The second one was on January 26, 1998, at 2227 UT from 15°S, 55°W associated with a CME at PA ∼260° (speed, ∼446 km s^{-1}). Although it is difficult to rule out the association between the type II bursts and the IP shock, the partial halo CME on January 25, 1998, at 1526 UT (from 25°N, 27°E) which had a WAVES type II burst (but no metric type II burst) seems to be the likely source for this shock.

3.6.6. May 2, 1998, MC. There were two metric type II bursts on April 29, 1998, that were temporally associated with this MC. The first one at 0813 UT did not have a CME event, but an EUV transient was detected at 0805 UT. The second one at 1622 UT (18°S, 20°E), associated with a fast CME (speed, 1016 km s^{-1}) at 1658 UT seems to be positively related to this MC. Another metric type II burst on May 1, 1998, at 0726 UT (associated with a CME at PA ∼57° moving with a speed of ∼503 km s^{-1}), was in the right time window but behind the east limb. It is unlikely that behind the limb event would result in an IP ejecta near Earth.

3.6.7. May 4, 1998, MC. The May 1, 1998, metric type II burst discussed above is in the correct time window, but the position is not appropriate. The May 2, 1998, halo CME at 1406 UT seems to be the solar source for this MC. This halo CME was not associated with a metric type II burst but produced complex, multiple episodes of a DH type II burst as detected by Wind/WAVES.

3.6.8. May 15, 1998, S. The type II burst at 0324 UT on May 14, 1998 (west limb event, CME at PA ∼265°, speed, ∼373 km s^{-1}), is too close in time; the transit time would be only 34 hours. For a limb CME like this, the projection effect is minimal so the measured plane of the sky speed (373 km s^{-1}) is expected to be close to the space speed. Such a CME would take about 4 days to reach 1 AU [*Gopalswamy et al.*, 2000a]. The CME-driven shock itself would arrive ∼0.5 days before the CME. Thus the expected transit time of 3.5 days is too large compared with the 34-hour time difference between the IP shock and metric type II burst. The correct solar event associated with the MC in question is therefore not the type II associated eruption, but the May 11, 1998, CME at 2155 UT with DSF close to the west limb. No metric type II burst, but a DH type II burst, was associated with this CME.

Thus the total number of positive associations between metric type II bursts and IP events is 10 out of 49 (20%). In all the cases with positive association, however, a large-scale CME was involved. A large-scale CME seems to be an essential requirement for a metric type II burst to be associated with an IP event. One may conclude that only shocks driven by large-scale CMEs (wider and faster) propagate all the way to 1 AU after originating from near the Sun.

3.7. Starting With DH Type II Bursts

The DH burst sources are typically located between the kilometric and metric domains. We start with the list of DH type II bursts and search for the metric counterparts on the one hand and kilometric and IP events on the other. The DH type II bursts in the spectral range 1-14 MHz could still be considered as near-Sun manifestations, because the heliocentric distances to the source regions of these bursts seem to be 2-4 R_s [*Reiner and Kaiser*, 1999]. There were in all 27 events in the DH domain during our study period (see Table 3). All but one of them were type II bursts. The May 3, 1998, event, a type IV burst, was the exception. We have listed the dates and onset times of the DH bursts in column 2, while their association with metric and kilometric type II bursts is indicated in columns 3 and 4 (N for no; Y for yes). CMEs (columns 5-7) and flares (columns 8-10) associated with the DH type II bursts are also listed. In the last column we have listed the associated IP event (S, MC, or E). *Gopalswamy et al.* [2000b] studied 25 of these events and determined the characteristics of solar eruptions that resulted in DH type II bursts. Here we discuss only the metric and IP consequences of the DH type II bursts. Table 3 contains two additional events not given by *Gopalswamy et al.* [2000b]. These two events were found retroactively (the 2153 UT event on September 23, 1997, and the 0115 UT event on June 22, 1998). Both of these events occurred close to the limb, and the IP ejecta were not detected. However, an IP shock associated with the June 22, 1998, event was detected in situ on June 25, 1998, and is listed in Table 2.

From the solar sources identified and listed in column 8 of Table 3, we can see that the DH type II events are evenly split between limb (13) and disk (14) events. As before,

we regard an event to be a disk event if the central meridian distance of the associated solar source is <60°. The single type IV burst on May 3, 1998, is a disk event. Out of the 14 disk events, seven (50%) had IP signatures and only eight (62%) had metric type II bursts. Out of the 13 limb DH type II bursts, similar fractions were associated with metric type II bursts (9/13, or ∼69%) and IP events (7/13, or ∼54%). The limb DH type II bursts seem to have a slightly better association with metric type II bursts, but the sample is not large enough to make a strong case. The fraction of kilometric type II bursts associated with DH type II bursts is also similar for the limb (7/13, or ∼54%) and disk (7/14, or 50%) events. If we exclude the type IV event, then all associations are evenly split between the limb and disk cases.

Thus, out of the 27 DH events, 14 (52%) had 1-AU counterparts. Only four of these 1-AU counterparts were IP ejecta, and the remaining 10 were "driverless shocks." This means even some disk eruptions produced only a shock signature near Earth. We can identify these disk eruptions in Table 3 as the CMEs on January 21, 1998 (57°S, 19°E), January 25, 1998 (24°N, 27°E) and April 27, 1998 (16°S, 50°E). The average distances from the disk center of those solar eruptions that result in IP ejecta were found to be 28° (longitude) and 17° (latitude) [*Gopalswamy et al.*, 2000a] (see also *Bravo and Blanco-Cano* [1998], who found an average central meridian distance of ∼30°). Note that the January 21, 1998, event occurred too far to the south to be intercepted by the spacecraft. The April 27, 1998, event had a longitude of 50°E and hence can be regarded as a limb event [*Gopalswamy et al.*, 1999a]. The January 25, 1998, event was relatively close to the disk center, but it was a filament eruption event; the preeruption filament was quiet extended toward the east limb and the associated CME appeared mostly over the east limb [*Gopalswamy et al.*, 1999b]. Another interesting point is that roughly the same number of these "driverless" shocks originated from the east and west limbs, in contradiction to *Cane* [1985], who concluded that "shocks originating on the west limb do not reach the earth."

Interestingly, all the 10 metric type II bursts that had IP association (see Tables 1 and 2) belonged to this subset of 14 DH type II bursts with IP signatures. The four DH type II bursts without metric type II bursts started only in the RAD2 spectral domain (<14 MHz). Thus the association between type II bursts and IP events increases from 10/49 (20%) to 14/49 (29%) when we include those starting in the outer corona. When kilometric type II bursts are included, then the association between IP events with any one kind (metric, DH, or kilometric) of type II bursts increases further.

We must point out that only 14 of the 27 DH type II bursts were associated with kilometric type II bursts, while there were 51 kilometric type II bursts observed during the study period. The identification of the solar sources of all the kilometric type II bursts is beyond the scope of this paper. It is likely that many of the white-light CMEs that did not produce metric or DH type II bursts might start driving shocks far into the IP medium and produce kilometric radio bursts. An additional possibility is that kilometric type II bursts may be due to backside events such that the IP ejecta and shocks do not reach the spacecraft while the electromagnetic radiation does [*Gopalswamy et al.*, 2000b].

From Table 3 we can see that nearly half of the WAVES/DH type II events did not have IP signatures. This again could be a com-

bination of the two possibilities: (1) Some DH type II bursts are similar to metric type II bursts except that they occur at slightly larger heliocentric distances, and (2) shock flanks from limb CMEs are not extended enough to be intercepted by the spacecraft.

3.8. Summary of Observational Results

We started with observations that imply shocks in each of the three domains of the Sun-Earth space (the inner corona (from metric type II bursts), the middle corona (from DH type II bursts) and near Earth (from in situ observations)) and looked for counterparts in the other domains. We found the following:

1. Only a small fraction (9%) of metric type II bursts on the solar disk (central meridian distance $< 60°$) were associated with IP shocks. A slightly larger fraction of metric type II bursts were associated with DH type II bursts (18%) and kilometric type II bursts (25%, the upper limit).

2. Conversely, only a small fraction of IP shocks (20%) were associated with metric type II bursts even after relaxing the constraint on the central meridian distance. Note that there were 137 metric type II bursts in all and 46 IP shocks during the observing period, yet only 10 events had positive association between the two domains. The association between IP shocks and type II bursts increases slightly to 29% when DH type II bursts are included.

3. In virtually every case that had metric type II and IP event association, a large-scale (width $> 120°$) CME was involved.

4. A significant number of type II bursts originated in the DH and kilometric domains with no metric counterparts.

5. About half (50%) of the limb type II bursts were associated with slow CMEs (<500 km s^{-1}). However, the speeds of limb CMEs associated with type II bursts had a lower cutoff at ~250 km s^{-1}.

6. We could not identify a white-light CME for a significant fraction (34%) of the disk type II bursts. However, an EIT transient was observed in all these cases. No other IP signature DH or kilometric type II burst, IP ejecta, or IP shock was detected for these CME-less metric type II bursts.

4. An Explanation for the Observed Relationship Between Coronal and IP Shocks

The observed poor correlation between coronal and IP shocks may be attributed to the nature of the shock driver, the characteristics of the ambient medium through which the shock propagates, or a combination of the two. In paper 1, this issue was considered mainly from the point of view of shock drivers [see, e.g., paper 1; *Cliver et al.*, 1999]. In this section we present an alternative explanation based on the Alfven speed profile in the corona and in the IP medium. From in situ observations, we know that the Alfven speed is very low compared with the solar wind speed, so the solar wind speed is the primary characteristic speed in deciding shock formation.

In the equatorial low corona (<2 R_s), under solar minimum conditions, the solar wind is not fully formed. The relevant characteristic speed is therefore the Alfven speed (or the magnetosonic speed). Typical Alfven speed at the coronal base for a magnetic field of 1 G and a density of $\sim 5 \times 10^8$ cm^{-3} is ~175 km s^{-1} while the sound speed (V_S) is about 110 km s^{-1}. Since ${V_F}^2 = {V_A}^2 + {V_S}^2$, we

get the fast mode magnetosonic speed (V_F) as $\sim$207 km s^{-1}. On the other hand, the Alfven speed in active regions is much higher in the low corona. For example, for a 100-G field (typical of flaring regions) and a density of $\sim 3 \times 10^9$ cm^{-3}, V_A $\sim$4000 km s^{-1}. Therefore one needs a very large amplitude disturbance to form a shock above active regions, whereas considerably weaker disturbances can drive shocks in the quiet regions. As the disturbance associated with an energy release moves away from the active region, it will produce shocks wherever the speed of the disturbance exceeds the local V_F. It is therefore likely that the shocks first form at locations transverse to the radial direction because the disturbance is likely to find V_F there rather than directly above the active region (of course, this depends on how the density and magnetic fields fall off above the active region).

4.1. Radial Profile of the Fast Mode Speed

In order to get the V_F profile in the corona, we need the V_A and V_S profiles. For the coronal region of interest, we take V_S to be constant with distance (110 km s^{-1} for a 1.5-MK corona). To get the V_A profile, we need the density (n) and magnetic field (B) variations with radial distance. Recently, *Mann et al.*, [1999a] computed an Alfven speed profile to explain the relationship between EIT waves and metric type II bursts. We perform a similar computation, except for a density model that is consistent with the starting frequencies of metric type II bursts listed in Table 1. We also consider the V_A profile above flaring active regions, in addition to the quiet regions, because both regions may be relevant, depending on the place of origin, speed, and extent of the driving disturbances. For active regions, we use the Saito density model (*Saito et al.*, 1977),

$$n(r) = 10^8 \times (0.0136 r^{-2.14} + 1.68 r^{-6.13}), \quad (1)$$

with a multiplicative factor of 10 to normalize the density to be $\sim 3 \times 10^9$ cm^{-3} at the base of the active region corona. Here r is the radial distance from the Sun center, in units of solar radii. For the magnetic field above active regions, we use the distribution of *Dulk and McLean* [1978]:

$$B = 0.5 \times (r-1)^{-1.5}, \quad (2)$$

which gives a magnetic field of $\sim$177 G at the base of the active region corona. For the quiet corona, we use 3$\times$ Saito model which gives a density of 5×10^8 cm^{-3} at the coronal base near the equator as obtained by *Fludra et al.*, [1999]. The 3$\times$ Saito model is very similar to the model by *Leblanc et al.* [1998] which is valid for the entire Sun-Earth distance. Since our starting point for metric type II bursts is near the Sun, we have to normalize the density close to the coronal base, rather than at 1 AU, so we use the former. Within the region of interest ($<$10 R_s), the models differ very little. The density model of *Mann et al.* [1999b] could also be used, but it differs significantly at distances $<$2 R_s. We obtain the quiet Sun magnetic field profile based on magnetic flux conservation ($r^2 B(r) = \text{const}$):

$$B(r) = 2.2 \times r^{-2}, \quad (3)$$

which gives $\sim$5 nT (10^{-5} G) at 1 AU, typical of the quiet values measured by the Wind spacecraft. This relation also gives $B = 2.2$ G at r=1, as expected for quiet Sun fields. Combining the magnetic field and density profiles, we obtained V_A and hence the V_F profile plotted in Figure 3a. For the active region case, V_F starts with a few thousand kilometers per second at the coronal base

and attains the quiet Sun value at $\sim$1.4 R_s and then rapidly falls below the quiet Sun value. This roughly corresponds to the metric corona where the active region blends with the background streamer belt [*Lantos et al.*, 1987]. For the quiet corona, V_F starts with a low value of $\sim$230 km s^{-1} close to the base, increases up to $\sim$540 km s^{-1} at 3.5 R_s, and then slowly decreases. The peak of the V_F curve depends on the actual density and magnetic field values, but the shape of the curve remains the same. For example, *Mann et al.* [1999a] obtained a peak value of $\sim$800 km s^{-1} at $\sim$4 R_s.

4.2. Implications of the V_F Profile

We can divide the solar corona into three regions as marked in Figure 3a.

4.2.1. Region 1 (inner corona).. This region is close the surface ($<$1.4 R_s), where the active region (AR) plays a dominant role. In this region, V_F is low only in the quiet regions (adjacent to AR). Radially above the AR, V_F is very high. Thus disturbances exceeding a speed of $\sim$230 km s^{-1} may be super-Alfvenic and produce fast mode shocks in the quiet corona surrounding active regions. This might explain the nonradial location of high-frequency type II bursts [see, e.g., *Gopalswamy et al.*, 2000c].

4.2.2. Region 2 (middle corona).. For distances $>$1.4 R_s but less than $\sim$3 R_s, AR magnetic fields do not play a strong role, so shocks can form anywhere above the active region. In region 2, V_F sharply rises (both above and outside of active regions), so it becomes progressively more difficult to form shocks. Thus shocks in region 1 may easily become MHD waves in region 2 and dissipate. Only shocks with speed $>V_{Fmax}$ can travel beyond region 2. The lifetime of a shock thus critically depends on its initial speed. Another factor, of course, is the lifetime of the driver.

4.2.3. Region 3 (outer corona and beyond).. In the region to the right of V_{Fmax} in Figure 3a where the heliocentric distances are $>\sim$3 R_s, V_F decreases from its peak; shock formation once again becomes easier in region 3 because of the lower Alfven speed. At still larger distances the solar wind flow speed gains significance and eventually becomes the dominant characteristic speed [see, e.g., *Sheeley et al.*, 1997].

To give an example, a disturbance moving with a speed of 400 km s^{-1} in region 2 may drive a shock only until it reaches a height of $\sim$2 R_s. At this height the disturbance ceases to drive a shock. If the driver is a CME, it can again set up a new shock when it reaches a distance of $\sim$6 R_s where V_F falls to 400 km s^{-1}. The SOHO/EIT instrument has detected a number of transients (EIT waves) [*Thompson et al.*, 1998] with speeds in the range 100-500 km s^{-1} in the low corona [*Klassen et al.*, 2000]. Note that some of these EIT transients have speeds high enough to be regarded as fast mode shocks in region 1. Consistent with this conclusion, simultaneous imaging observations in radio and EUV have shown that the metric type II burst is spatially coincident with the EIT wave [*Gopalswamy et al.*, 2000c]. When these disturbances continue to propagate outward, they face higher and higher Alfven speed, so whenever their speed equals local V_F, they cease to be shocks. *Mann et al.* [1999a] have interpreted the EIT waves as fast mode waves in the preshock stage of coronal shocks responsible for type II bursts.

In Figure 3b we have compared the plasma frequency profiles (from equation (1)) corresponding to the quiet region (dash-dotted) and active region (dashed curve) corona with

the V_F profile. Note that most of the starting frequencies listed in Table 1 correspond to distances $<1.75R_s$. Since V_F sharply increases in this region, many shocks might weaken and die off in this region. This is also the region where most metric type II bursts seem to die off. Note that the WAVES/RAD2 spectral range (14-1 MHz) roughly starts in region 3 at $\sim 3R_s$, close to the peak of the V_F profile. Therefore only disturbances with speeds exceeding V_{Amax} can produce DH type II bursts. However, at larger distances, slightly slower disturbances can drive shocks. CMEs are the main solar disturbances observed by coronagraphs at coronal heights corresponding to DH type II bursts. *Gopalswamy et al.* [2000b] found that all the DH type II bursts were associated with CMEs and that the CMEs were faster and wider than the average. The V_F profile provides a natural explanation for those type II bursts that start in the DH domain without a metric counterpart. In these cases the responsible CME starts off slow and accelerates to attain super-Alfvenic speed only at distances corresponding to the DH domain. Examples of this population of type II bursts were discussed earlier in section 3.7. Faster CMEs ensure that the shocks are super-Alfvenic, while wider CMEs increase the chance of finding some coronal region where the CMEs are super-Alfvenic. If CMEs are fast enough at low enough heights, they can also drive shocks in region 2. The May 19, 1998, CME in Table 1 is a good example which produced metric and DH type II bursts.

In summary, the V_F profile in Figure 3a can explain most of the observed characteristics of metric, DH and kilometric type II bursts: (1) It is easy to produce metric type II bursts in the inner corona because V_F is very low. Only a small number of such shocks can continue beyond $\sim 3R_s$. (2) A long-lived driver, such as a CME, has more opportunity to produce a type II burst because it goes through a low V_F region especially in the outer corona. This means they can set up a shock anywhere in the corona so long as they move at super-Alfvenic speeds. (3) CMEs with intermediate speeds can drive shocks in the metric domain, lose the shock in the regions of V_{Amax}, and again set up a shock in the outer corona. (4) Accelerating, low-speed CMEs may produce shocks in the DH and kilometric domains even though they do not drive shocks in the metric domain. (5) Blast waves and shocks driven by short-lived drivers have less chance to go beyond the metric domain, unless their initial speed exceeds V_{Amax}.

While deriving the V_F profile, we had assumed that quantities vary smoothly with radial distance. In the real corona and IP medium, inhomogeneities of various scales are present which may have significant effect on the shocks. For example, local density enhancements may strengthen a section of a weak shock that passes through the inhomogeneity. This is consistent with the patchiness often observed in the dynamic spectra of type II bursts.

5. Discussion

5.1. Comparison With Past Results

We considered a large number of IP events detected near Earth during a 44-month period from November 1994 to June 1998 and their counterparts at various subregions between the Sun and Earth. The number of IP ejecta (49) is large enough to be compared with many of the past studies involving IP ejecta. We note that most of the IP ejecta in our list were driving shocks: 33/36 (92%). If we consider MCs alone, the percentage is

similar: 27/29 (93%). Thus the fraction of IP ejecta driving shocks is much larger than in previous reports. *Klein and Burlaga* [1982] reported that only 30% of magnetic clouds identified during the period 1967-1978 were driving shocks. Much higher percentages of MCs observed during 1978-1982 were found to be driving shocks in two later studies (80% in the study of *Zhang and Burlaga* [1988] and 70% in that of *Marsden et al.* [1987]). The percentage of association in our study is closest to but significantly larger than that of *Zhang and Burlaga* [1988].

The only study to our knowledge that considered the association between IP ejecta and metric type II bursts is by *Wilson and Hildner* [1984]. These authors found that six out of nine MCs with shocks (67%) had metric type II association. In our case, only 4/36 IP ejecta (11%) were associated with metric type II bursts, despite a wider window of longitudes used by us (60° versus 49°). If we consider only those ejecta and MCs driving shocks at 1 AU, the percentage (12%) is still nowhere near what *Wilson and Hildner* [1984] found. In fact, one of the MCs in our list associated with a metric type II burst was not driving a shock at 1 AU (event 43 in Table 2). If we consider MCs alone, only two were associated with metric type II bursts (2/26, or ∼8%). When we include all the IP events (assuming that the drivers of isolated shocks were CMEs but were not intercepted by Wind), their association with metric type II bursts (irrespective of the event longitude) improves slightly (10/49, or ∼20%). This again is not consistent with what *Wilson and Hildner* [1984] obtained. Thus the results of *Wilson and Hildner* [1984] seems to be due to an insufficient sample size.

Robinson et al. [1984] found that only a small fraction (16/240, or ∼6.7%) of metric type II bursts observed by the Culgoora radiospectrograph were followed by kilometric type II bursts for a 40-month period from September 1978 to December 1981. We find essentially the same result (10/137, or ∼7.3%), except that we compared shocks detected *in situ* with metric type II bursts. Since kilometric type II bursts are closely related to IP shocks detected in situ, the results are consistent. *Robinson et al.* [1984] examined the characteristics of the solar eruptions that resulted in metric type II bursts followed by kilometric type II bursts. They concluded that the IP type II bursts were associated with strong flare phenomenon, intense continuum radiation, metric type II bursts of low starting frequency, and herringbone structures. Our results mostly agree with *Robinson et al.*'s, [1984] result, except for X-ray importance and duration. Four of our end-to-end events had X-ray flare duration less than 30 min. The starting frequencies of metric type II bursts were also larger in our case: The lowest was 55 MHz, and most of the starting frequencies were in the normal range (60-250 MHz).

Cane and Stone [1984] used an expanded the list of *Robinson et al.* [1984] to include metric type II bursts from other observatories and found that ∼70% of the IP shocks were preceded by metric type II bursts. This certainly contradicts our findings. However, the comparison may not be meaningful because *Cane and Stone* [1984] did not use an exhaustive list of IP shocks (or kilometric type II bursts). In fact, their data selection was based on a subset of kilometric type II bursts that "has been restricted to those events which drift through the data at a rate consistent with known shock velocities...."

5.2. Metric Type II Bursts, CMEs, and Flares

The high degree of association between metric type II bursts, CMEs, and flares continues to be a puzzle [*Robinson et al.*, 1984; *Cane*, 1984; *Cane and Stone*, 1984; *Sheeley et al.*, 1985]. In the low corona it is not clear whether CMEs drive a shock or contribute in some way to shock formation (by providing higher-density medium or causing reconnection).

Even though LASCO is much more sensitive than previous coronagraphs, it did not detect CMEs during a significant fraction (11/32, or ∼34%) of disk metric type II bursts. Note that there were no IP events (DH type II, kilometric type II, or IP events, except for a kilometric type II which may be fortuitous) that were associated with CME-less type II bursts. While there is no doubt that almost all of the DH type II bursts are due to CMEs, the lack of CMEs in about a third of the metric type II bursts continues to pose a problem for the hypothesis that fast CMEs constitute the sole driver of all shocks [see also *Kahler et al.*, 1984]. Observability is a good explanation because we considered only disk events (central meridian distance $< 23°$). Only by studying a set of limb type II bursts without CMEs can one decide whether type II bursts occur without CMEs. We must point out that some of the CME-less type II bursts occurred when an earlier CME was in progress. It is not clear how this would affect the observability of the associated CME.

Presence of a fast CME has been suggested as the primary requirement for the occurrence of a metric type II burst, and not the low Alfven speed in the flaring region [*Cliver et al.*, 1999]. The definition of fast CMEs is not very clear, especially with reference to Figure 1 where we can see that half of the type II associated limb CMEs have speeds less than 500 km s^{-1}: Is this fast relative to coronal Alfven speed or to solar wind speed? From Figure 1c we see that limb CMEs with metric type II bursts have a lower cutoff of ∼250 km s^{-1}, which is larger than the minimum value of the fast mode speed in the corona (see Figure 3a). This means that if the CMEs were to drive the shocks, they need to have speeds ∼250 km s^{-1} very close to the surface (<1.4 R_s).

As we saw in Figure 3a, one has to consider the Alfven speed not only in the flaring region, but also outside, where the condition for shock formation is favorable especially for type II bursts of high starting frequency. In Table 1 the maximum starting frequency is 350 MHz (the September 25, 1997, event), corresponding to a local plasma density of $\sim 1.5 \times 10^9$ cm^{-3}. Such high-frequency type II bursts are not uncommon [see, e.g., *Vrsnak et al.*, 1995], but the corresponding plasma densities exist only in active regions, close to the flare site. For a 10× Saito model and a magnetic field distribution given by (2), the Alfven speed exceeds 6000 km s^{-1}. Thus the shock has to form at the periphery of the active region where the Alfven speed is relatively low. Note that the plasma frequency at the quiet coronal base is ∼200 MHz, so the 350-MHz plasma level has to be in the active region. An estimate of shock speed for this type II burst was made by *Klassen et al.* [2000] to be ∼1000 km s^{-1}. The associated flare occurred from AR 8088 at S28E04, but no CME was reported. The SOHO/EIT detected a brow type wave at ∼1156 UT while the type II bursts started at 1146.9 UT, close to the peak of a hard X-ray flare at 1146.1 UT. It is unclear at present if a CME could be moving with such a high speed almost at the coronal base. If CMEs are responsible for

such high-frequency type II bursts, they have to start out with very small volume close to the coronal base. *Dere et al.* [1997] have reported on such a CME, but it was not associated with a CME. On the other hand, CMEs involving transequatorial loops are of large scale inherently. It is now possible to measure CME speeds close to the solar surface using SOHO/LASCO C1 and EIT data, and fast CMEs were found to accelerate similarly to the slow ones, but at much lower coronal heights [*Gopalswamy and Thompson*, 2000]. Therefore it should be possible to decide if the CMEs have speeds exceeding V_F. However, we cannot say whether CMEs are the sole source of all metric type II bursts, especially because of other sources of mass motion close to the flare site such as chromospheric evaporation, hot X-ray plasmoids, and reconnection jets. Speeds of many of these objects can easily exceed the local Alfven speed in the periphery of active regions [*Gopalswamy, et al.*, 1997].

5.3. Implications to Shock Forecasting

Although there are numerical models being used to predict the arrival of shocks at 1 AU based on metric type II bursts and flares, the present study as well as paper 1 have shown that the correspondence between IP and coronal shocks (inferred from metric type II bursts), is extremely poor. Even if we consider DH type II bursts as the extreme case of the low-starting frequency metric type II bursts, we see that only 14/46 shocks could be accounted for this way. This is still only 30% of all the IP shocks. Thus, starting with metric type II bursts (or coronal shocks) it is extremely difficult to predict the IP shocks. Numerical models have been developed to predict the arrival of IP shocks with input from metric type II burst observations. The "shock-time-of-arrival" (STOA) model is one such, claimed to be able to "predict the approximate location and time of arrival of the IPS disturbances" [*Ananthakrishnan et al.*, 1999]. Validity of this model has been questioned in paper 1 and by *Kadinsky-Cade et al.* [1998]. The poor association between metric type II bursts on the disk and IP shocks detected in situ is not supportive of the STOA model.

6. Conclusions

We compared 137 metric type II bursts and 49 IP events over a period of 44 months from November 1994 to June 1998. Imposing the constraint that the near-Sun and near-Earth manifestations should be within 5 days, only 10 events overlapped. If we include type II bursts in the decameter-hectometric domain, the association slightly improved to 14 events. The small fraction of metric type II bursts that did have IP association invariably involved large-scale (halo) CMEs. Coupled with the fact that most of the IP events were associated with large-scale CMEs (halo or partial halo), we conclude that the large-scale CME is the primary near-Sun activity that significantly disturbs the solar wind [see also *Gosling*, 1993]. The poor correlation between metric type II bursts and IP shocks suggests that numerical models based on metric type II bursts to predict the shock arrival time at 1 AU are questionable, as we pointed out in paper 1.

A significant number (12/46, or ~26%) of isolated IP shocks (without drivers) were detected. In all these cases, limb CMEs (ejected transverse to the Sun-Earth line) were found near the Sun, suggesting that the IP shocks had much larger extent than the drivers. The white-light CMEs associated with these iso-

lated shocks were also of large width: Most of them were halo or partial halo events. Eruptions from both the limbs produced shock signatures at Earth, contradicting an earlier conclusion by *Cane* [1985] that west limb eruptions do not result in shocks at Earth. The "driverless" shocks also had better type II radio burst association: 50% with metric type II bursts and 92% with DH type II bursts. This is a significant result, but the sample size is small. We need more isolated shocks to confirm this result.

Since almost all DH and kilometric type II bursts as well as in situ detected shocks are associated with CMEs, it is tempting to conclude that the metric type II bursts are also associated with CMEs. However, we continue to see that a third of the metric type II bursts are not associated with CMEs. Furthermore, the type II bursts without CMEs were not followed by type II bursts in the DH or kilometric domains; they were not followed by any IP events either.

The Alfven (or magnetosonic) speed profile in the corona and its latitudinal dependence may play a crucial role in understanding the relation between coronal and IP shocks. There is a distinct possibility that the same driver can cause different shocks at different distances from the Sun depending on the radial profiles of Alfven and CME speeds. However, this does not rule out other possible drivers close to the Sun where it seems to be very easy to drive shocks.

Acknowledgments. We thank D. Berdichevsky, R. P. Lepping, and A. Szabo for their help in preparing the IP signature list and O. C. St. Cyr for LASCO data. This research was supported by NASA (NCC5-376, NCC5-418, and NAG5-8998), AFOSR (F49620-00), and NSF (ATM9819924) grants to the Catholic University of America.

Janet G. Luhmann thanks Silvia Bravo and another referee for their assistance in evaluating this paper.

References

Acuña, M. H., K. W. Ogilvie, D. N. Baker, S. A. Curtis, D. H. Fairfield, and W. H. Mish, The global geospace program and its investigations, *Space Sci. Rev., 71*, 5, 1995.

Ananthakrishnan, S., M. Tokumaru, M. Kojima, V. Balasubramanian, P. Janardhan, P. K. Manoharan, and M. Dryer, Study of solar wind transients using IPS, in *Solar Wind Nine*, edited by S. Habbal et al., *AIP Conf. Proc., 471*, 321, 1999.

Bougeret, J-L., et al., Waves: The radio and plasma wave investigation on the Wind spacecraft, *Space Sci. Rev., 71*, 231, 1995.

Bravo, S., and X. Blanco-Cano, Signature of interplanetary transients behind shocks and their associated near-surface activity, *Ann. Geophys., 16*, 359, 1998.

Brueckner, G.E., et al., The large angle spectroscopic coronagraph (LASCO), *Sol. Phys., 162,* 357, 1995.

Burlaga, L., E. Sittler, F. Mariani, and R. Schwenn, Magnetic loop behind an interplanetary shock: Voyager, Helios, and IMP 8 observations, *J. Geophys. Res., 86*, 6673, 1981.

Cane, H, V., The relationship between coronal transients, type II bursts and interplanetary shocks, *Astron. Astrophys., 140*, 205, 1984.

Cane, H. V., The evolution of interplanetary shocks, *J. Geophys. Res., 90*, 191, 1985.

Cane, H. V. and R. G. Stone, Type II solar radio bursts, interplanetary shocks, and energetic particle events, *Astrophys. J., 282*, 339, 1984.

Cane, H. V., N. R. Sheeley, and R. A. Howard, Energetic interplanetary shocks, radio emission, and coronal mass ejections, *J. Geophys. Res., 92*, 9869, 1987.

Cliver, E. W., D. F. Webb, and R. A. Howard, On the origin of solar metric type II bursts, *Sol. Phys., 187*, 89, 1999.

Delaboudinière, J. P., et al., EIT: extreme-ultraviolet imaging telescope for the SOHO Mission, *Sol. Phys., 162*, 291, 1995.

Dere, K. P. et al., EIT and LASCO observations of the initiation of a coronal mass ejection, *Solar Phys., 175*, 601, 1997.

Dulk, G. A., and D. J. McLean, Coronal magnetic fields, *Astron. Astrophys., 66*, 315, 1978.

Fludra, A., G. Del Zanna, D. Alexander, and B. J. I. Bromage, Electron density and temperature of the lower solar corona, *J. Geophys. Res., 104*, 9709, 1999.

Gopalswamy, N. and B. J. Thompson, Early life of coronal mass ejections, *J. Atmos. Sol. terr. Phys., 62*, 1457, 2000.

Gopalswamy, N., M. R. Kundu, P. K. Manoharan, A. Raoult, N. Nitta, and P. Zarka, X-ray and radio studies of a coronal eruption: Shock wave, plasmoid and coronal mass ejection, *Astrophys. J., 486*, 1036, 1997.

Gopalswamy, N., M. L. Kaiser, R. P. Lepping, S. W. Kahler, K. Ogilvie, D. Berdichevsky, T. Kondo, T. Isobe, and M. Akioka, Origin of coronal and interplanetary shocks: A new look with Wind spacecraft data, *J. Geophys. Res., 103*, 307, 1998.

Gopalswamy, N. M. L. Kaiser, R. J. MacDowall, M. J. Reiner, B. J. Thompson, and O. C. St. Cyr, Dynamical phenomena associated with a coronal mass ejection, in *Solar Wind Nine*, edited by S. Habbal et al., *AIP Conf. Proc., 471*, 641, 1999a.

Gopalswamy, N., S. Yashiro, M. L. Kaiser, B. Thompson, S., and S. Plunkett, Multi-wavelength signatures of a coronal mass ejection, in *Solar Physics With Radio Observations*, edited by T. Bastian, N. Gopalswamy, and K. Shibasaki, *Rep. 479*, Nobeyama radio Obs., Nobeyama, Japan, 1999b.

Gopalswamy, N., A. Lara, R. P. Lepping, M. L. Kaiser, D. Berdichevsky, and O. C. St. Cyr, Interplanetary acceleration of coronal mass ejections, *Geophys. Res. Lett., 27*, 145, 2000a.

Gopalswamy, N., M. L. Kaiser, B. J. Thompson, L. Burlaga, A. Szabo, A. Lara, A. Vourlidas, S. Yashiro, and J.-L. Bougeret, Radio-rich solar eruptive events, *Geophys. Res. Lett., 27*, 1427, 2000b.

Gopalswamy, N., M. L. Kaiser, J. Sato, and M. Pick, Shock wave and EUV transient during a flare, in *High Energy Solar Physics: Anticipating HESSI, ASP Conf. Ser.*, edited by R. Ramaty and N. Mandzhavidze, *406*, 351, 2000c.

Gosling, J. T., The solar flare myth, *J. Geophys. Res., 98*, 18,937, 1993.

Gosling, J. T., E. Hildner, R. M. MacQueen, R. H. Munro, A. I. Poland, and C. L. Ross, The speeds of coronal mass ejection events, *Sol. Phys., 48*, 389, 1976.

Howard, R. A., D. J. Michels, N. R. Sheeley, and M. J. Koomen, The observations of a coronal transient directed at Earth, *Astrophys. J., 263*, L101, 1982.

Kadinsky-Cade, K., S. Quigley, and G. Ginet, Validation of interplanetary shock propagation models (abstract), *EOS Trans. AGU, 79*(45), Fall. Meet. Suppl., F712, 1998.

Kahler, S. W., N. R. Sheeley, R. A. Howard, and M. J. Koomen, Characteristics of flares producing metric type II bursts and coronal mass ejections, *Sol. Phys., 93*, 33, 1984.

Kaiser, M. L., M. J. Reiner, N. Gopalswamy, R. A. Howard, O. C. St. Cyr, B. J. Thompson, and J.-L. Bougeret, Type II radio emissions in the frequency range 1-14 MHz associated with the April 7, 1997, solar event, *Geophys. Res. Lett., 25*, 2501, 1998.

Klassen, A., H. Aurass, G. Mann, and B. J. Thompson, Catalogue of the 1997 SOHO-EIT coronal transient waves and associated type II radio burst spectra, *Astron. Astrophys. Suppl. Ser., 141*, 357, 2000.

Klein, L. W., and L. Burlaga, Interplanetary magnetic clouds at 1 AU, *J. Geophys. Res., 87*, 613, 1982.

Lantos, P., C. E. Alissandrakis, T. E. Gergely, and M. R. Kundu, Quiet Sun and slowly varying component at meter and decameter wavelengths, *Sol. Phys., 112*, 325, 1987.

Leblanc, Y., G. A. Dulk, and J.-L. Bougeret, Tracing the electron density from the corona to 1 au, *Solar Phys., 183*, 165, 1998.

Lepping, R. P., et al., The WIND magnetic field investigation, *Space Sci. Rev., 71*, 207, 1995.

Mann, G., H. Aurass, A. Klassen, C. Estel, and B. J. Thompson, Coronal transient waves and coronal shock waves, in *Plasma Dynamics and Diagnostics in the Solar Transition Region and Corona*, edited by J.-C. Vial and B. Kaldeich-Schurmann, *ESA SP-446*, 477, 1999a.

Mann, G., F. Jansen, R. J. MacDowall, M. L. Kaiser, and R. G. Stone, A heliospheric density model and type III radio bursts, *Astron. Astrophys., 348*, 614, 1999b.

Marsden, R. G., T. R. Sanderson, C. Tranquille, K.-P. Wenzel, and E. J. Smith, ISEE 3 observations of low-energy proton bidirectional events and their relation to isolated interplanetary magnetic structures, *J. Geophys. Res., 92*, 11,009, 1987.

Munro, R. H., J. T. Gosling, E. Hildner, R. M. MacQueen, A. I. Poland, and C. L. Ross, The association of coronal mass ejection transients with other forms of solar activity, *Solar Phys., 61*, 201, 1979.

Ogilvie, K. W., et al., SWE, a comprehensive plasma instrument for the Wind spacecraft, *Space Sci. Rev., 71*, 55, 1995.

Reiner, M. J., and M. L. Kaiser, High-frequency radio emissions associated with shocks driven by coronal mass ejections, *J. Geophys. Res., 104*, 16,979, 1999.

Reiner, M. J., M. L. Kaiser, N. Gopalswamy, H. Aurass, G. Mann, A. Vourlidas, and M. Maksimovich, Statistical analysis of coronal shock dynamics implied by radio and white-light observations, *J. Geophys. Res.*, this issue.

Robinson, R. D., R. T. Stewart, and H. V. Cane, Properties of metre-wavelength solar bursts

associated with interplanetary type II emission, *Sol. Phys., 91*, 159, 1984.

Saito, K., A. I. Poland, and R. H. Munro, A study of the background corona near solar minimum, *Solar Phys., 55*, 121,1977.

Sheeley, N. R., Jr., R. A. Howard, M. J. Koomen, D. J. Michels, R. Schwenn, K. H. Mulhauser, and H. Rosenbauser, Coronal mass ejections and interplanetary shocks, *J. Geophys. Res., 90*, 163, 1985.

Sheeley, N. R., Jr., et al., Measurements of flow speeds in the corona between 2 and 30 $R_{\odot}$, *Astrophys. J., 484*, 472, 1997.

St. Cyr, O. C., et al., Properties of coronal mass ejections: SOHO LASCO observations from January 1996 to June 1998, *J. Geophys. Res., 105*, 18,169, 2000.

Thompson, B. J., S. P. Plunkett, J. B. Gurman, J. S. Newmark, O. C. St. Cyr, and D. J. Michels, SOHO/EIT observations of an Earth-directed coronal mass ejection on May 12, 1997, *Geophys. Res. Lett., 25*, 2465, 1998.

Vrsnak, B., V. Ruzdjak, P. Zlobec, and H. Aurass, Ignition of MHD shocks associated with solar flares, *Sol. Phys., 158*, 331, 1995.

Wilson, R. M., and E. Hildner, Are interplanetary magnetic clouds manifestations of coronal transients at 1 AU?, *Sol. phys., 91*, 169, 1984.

Zhang, G., and L. F. Burlaga, Magnetic clouds, geomagnetic disturbances, and cosmic ray decreases, *J. Geophys. Res., 93*, 2511, 1988.

J.-L. Bougeret, 5, Place Jules Janssen, Meudon Principal Cedex, Meudon, France

N. Gopalswamy, Center for Solar Physics and Space Weather, The Catholic University of America, Washington, D. C. 20064. (gopals@fugee.gsfc.nasa.gov)

M. L. Kaiser, Bldg 2, Room 103, Code 695.0, NASA Goddard Space Flight Center, Greenbelt, MD 20771

A. Lara, Instituto de Geofisica, UNAM, Mexico City, Mexico

Received June 2, 2000; revised August 2, 2000; accepted August 2, 2000.

[1]Center for Solar Physics and Space Weather, The Catholic University of America, Washington, D. C.

[2]Also at NASA Goddard Space Flight Center, Greenbelt, Maryland

[3]Instituto de Geofisica, UNAM, Mexico City, Mexico

[4]NASA Goddard Space Flight Center, Greenbelt, Maryland

[5]University of Paris, Departement de Recherche Spatiale, Meudon, France

This preprint was prepared with AGU's LaTeX macros v5.01. File cua˙conf formatted August 31, 2001.

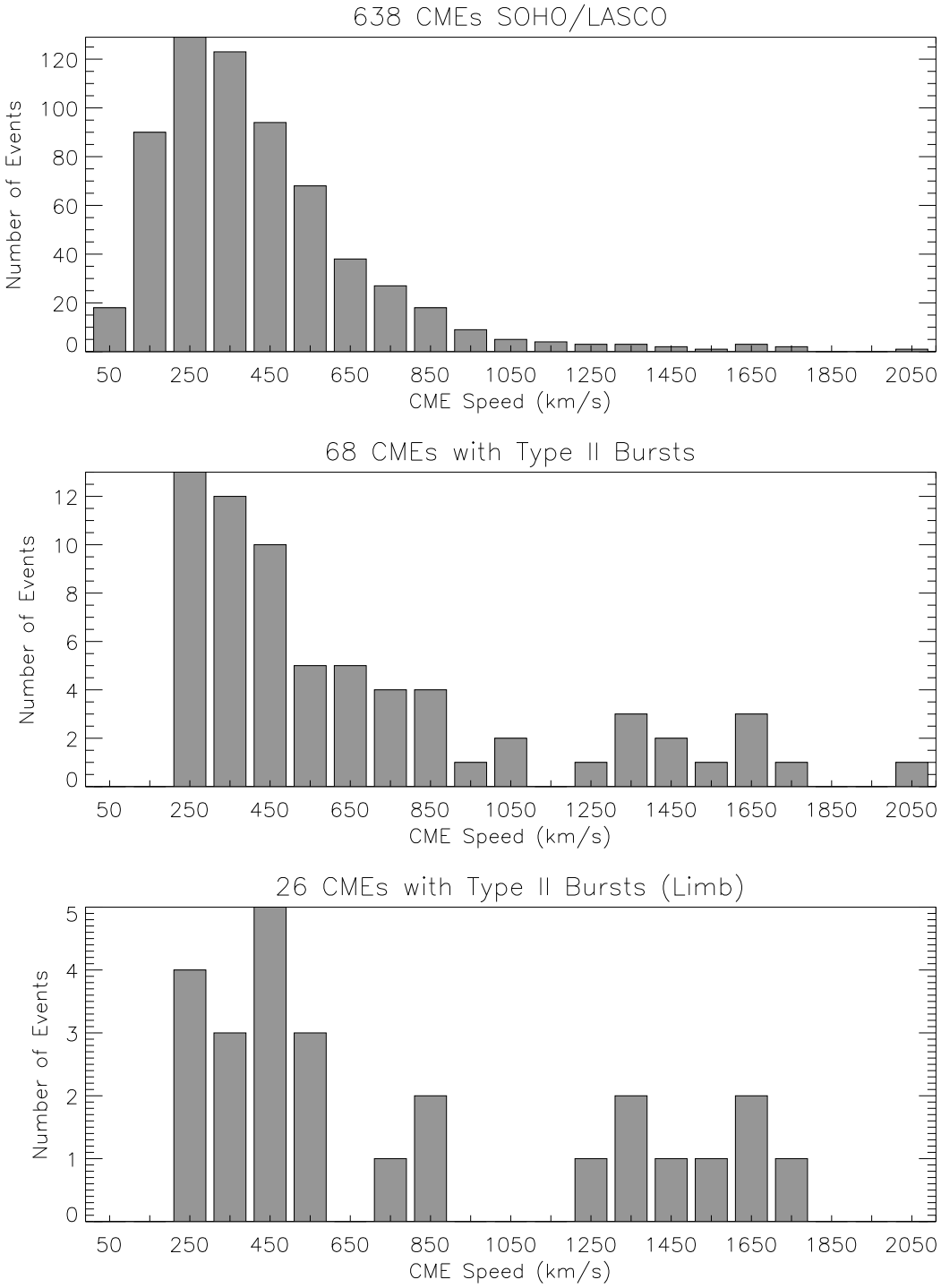

Figure 1. Histogram of coronal mass ejection (CME) speeds for (a) all CMEs, (b) all CMEs with metric type II bursts and (c) for CMEs associated with limb type II bursts.

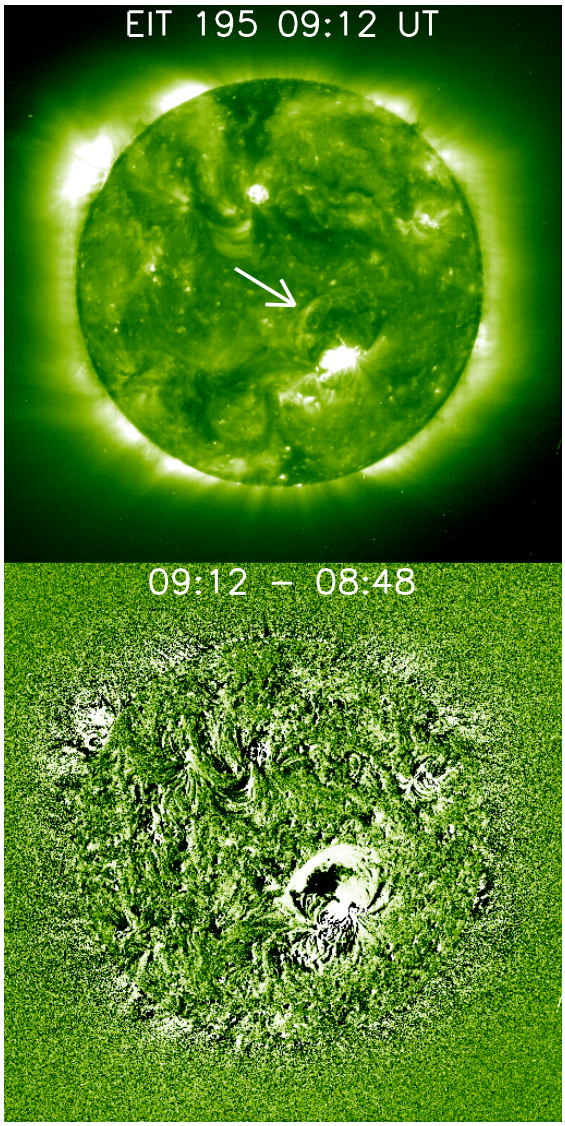

Figure 2. (top) An extreme-ultraviolet imaging telescope image at 0912 UT and (bottom) its difference with a preevent image at 0848 UT (at right) showing a "brow wave" on November 3, 1997. An arrow points to the brow in the undifferenced image.

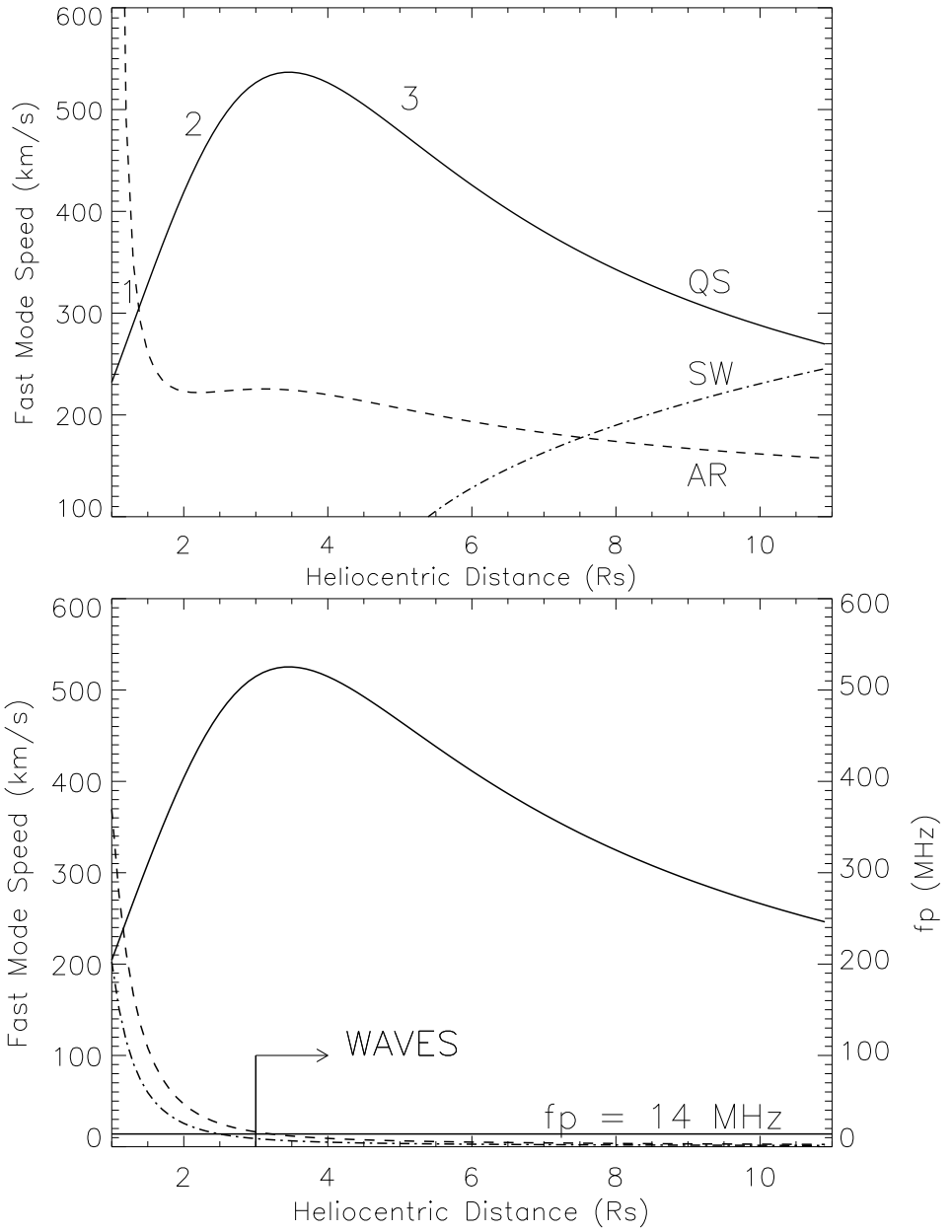

Figure 3. (a) Speed profile of the fast magnetosonic mode in the quiet Sun (solid line) and active region (dashed line) coronas. Three regions 1, 2, and 3 are marked where the conditions for shock formation are different. Solar wind speed profile from Sheeley et al. [1997] (dash-dotted line) is added for comparison. (b) Speed profile of the fast mode in the quiet corona (solid line) along with plasma frequency (f_p) profiles for 10× (dashed line) and 3× (dash-dotted line) Saito models corresponding to the quiet and active region coronas, respectively. The plasma frequency corresponding to the upper edge (14 MHz) of the WAVES/RAD2 receiver is marked.

Table 1. List of Metric Type II Bursts from Longitude $\leq 60^o$

No.	Date	Type II		GOES	Location	AR	Flare	CME	IP Event		
		f_s	UT	time			importance	speed[a]	DH	km	Ejecta
1	Nov 27, 1994	70	1628	1611-1619	S16W26	7811	C2.2/1N	ND	N	N	N
2	Dec 14, 1994	100	0547	0541-0554	S10W07	7815	M1.5/1N	ND	N	N	N
3	Dec 19, 1994	180	0439	0436-0454	N00E49	7817	C4.1/1M	ND	N	12/23	N
4	Feb 02, 1995	90	1309	1255-1328	S14E35	7834	C7.4/SB	ND	N	N	N
5	Feb 03, 1995	130	0155	0138-0214	S14E32	7834	M4.3/2B	ND	N	N	N
6	Feb 04, 1995	75	1547	1542-1639	S16E09	7834	M2.6/2B	ND	N	N	MC/S 02/08?
7	Feb 20, 1995	45	0328	0313-0342	N10E31	7844	M1.1/1N	ND	N	N	N
8	Feb 21, 1995	50	0740	0720-0801	N14E15	7844	C3.2/SN	ND	N	N	N
9	Mar 18, 1995	60	1922	1920-1943	S16E16	7854	B5.4/SF	ND	N	N	N
10	Mar 29, 1995	46	0654	0648-0700	S13E07	7858	C1.6/SF	ND	N	4/1	N
11	Oct 13, 1995	245	0504	0501-0516	S11E43	7912	M4.8/1F	ND	N	N	N
12	Jul 09, 1996	220	0911	0503-0548	S11W30	7978	C3.8/SF	426	N	N	N
13	Apr 01, 1997	85	0503	0456-0526	S26E22	8026	C4.0/SB	374	N	N	N
14	Apr 01, 1997	95	0801	0752-0804	S25E20	8026	C2.2/SF	N	N	N	N
15	Apr 01, 1997	80	1031	1023-1038	S25E20	8026	C2.1	N	N	N	N
16	Apr 01, 1997	135	1349	1342-1408	S25E16	8026	M1.0/1B	296	Y	N	N
17	Apr 02, 1997	50	0527	0524-0537	S25E05	8026	C1.3/SF	338	N	N	N
18	Apr 02, 1997	65	0938	0920-0933	S24E07	8026	B6.8/SF	N	N	N	N
19	Apr 07, 1997	125	1358	1350-1419	S30E19	8027	C6.8/3N	830H	Y	4/7	E/S 04/11
20	Apr 15, 1997	125	1415	1400-1426	S23E11	8032	C1.0	N	N	N	N
21	May 12, 1997	60	0454	0442-0526	N21W08	8038	C1.3	306H	Y	5/14	MC/S 5/15
22	May 21, 1997	70	2010	2003-2027	N05W12	8040	M1.3/SF	303	N	5/21	N
23	Jul 25, 1997	70	2024	2005-2230	N16W54	8065	C4.0/SF	632	N	N	N
24	Sep 12, 1997	76	1605	1603-1611	N23W18	8084	B5.0/SF	DG	N	N	N
25	Sep 24, 1997	60	0249	0243-0252	S31E19	8088	M5.9/1B	N	N	N	N
26	Sep 24, 1997	225	1103	1057-1110	S28E18	8088	M3.0/SF	350	N	N	N
27	Sep 24, 1997	70	1834	1824-1845	S29E15	8088	C8.3/1N	N	N	N	N
28	Sep 25, 1997	350	1147	1140-1155	S27E02	8088	C7.2/1N	N	N	N	N
29	Oct 09, 1997	45	1158	1147-1218	N24E35	8092	B9.2/SF	233	N	N	MC/S 10/10?
30	Oct 11, 1997	80	0850	0842-0911	N22E14	8092	B4.8/SF	320	N	N	N
31	Nov 03, 1997	130	0437	0432-0449	S20W13	8100	C8.6/SB	297	Y	11/3	MC/S 11/07?
32	Nov 03, 1997	125	0908	0903-0910	S20W15	8100	M1.4/1B	N	N	N	MC/S 11/07?
33	Nov 03, 1997	100	1026	1018-1034	S20W15	8100	M4.2	366	Y	N	MC/S 11/07?
34	Nov 04, 1997	60	0558	0552-0602	S14W33	8100	C2.1/2B	830H	Y	11/5	MC/S 11/07
35	Nov 04, 1997	50	1126	1124-1151	N22E14	8103	C1.0/SF	N	N	N	MC/S 11/07?
36	Jan 27, 1998	95	2215	2212-2245	N12E20	8144	B2.0	N	N	N	N
37	Apr 02, 1998	179	1617	1611-1737	S23E23	8190	C1.8/SF	333	N	4/3	N
38	Apr 27, 1998	30	0908	0855-0938	S16E50	8210	X1.0/2B	1631	Y	4/28	N
39	Apr 29, 1998	70	0831	0745-0827	S17E23	8210	C1.7/1F	N	N	5/1	MC 05/02?
40	Apr 29, 1998	50	1622	1606-1659	S18E20	8210	M6.8/3B	1016H	N	5/1	MC 05/02
41	May 06, 1998	80	2339	2327-0002	N28W36	8214	M2.5/SF	216	N	5/7	N
42	May 19, 1998	80	0951	1010-1018	N29W46	-	B7.9	796	N	N	Y
43	Jun 20, 1998	135	1421	1412-1444	N13W23	8243	C4.0/1N	286	Y?	N	MC 6/24?
44	Jun 22, 1998	45	0436	0427-0501	N16W46	8243	C2.9/SF	204	Y?	N	MC 6/24?

ND = no data; DG = data gap; $\mathbf{f_s}$ = starting frequency in MHz; AR = active region; MC = magnetic cloud; km = kilometric

[a]km s^{-1}

Table 2. IP Signatures (Magnetic Clouds, Ejecta and Shocks)

No.	Date (hr)	Object	Speed (km/s)	Radio burst m	DH	km	Solar source	Location	CME speed
1	02/08/95 03	MC/S	410	*2/4	N	N	Many DSFs	-	ND
2	03/04/95 11	MC/S	443	N	N	Y	02/28-00:11 DSF	S09E36	ND
3	04/06/95 07	MC/S	334	N	N	N	04/04-22:02 DSF	S15W24	ND
4	05/13/95 11	MC/S	331	N	N	N	05/11-13:25 DSF	N10E36	ND
5	08/22/95 22	MC/S	360	N	N	N	08/18-11:52 DSF	N30W04	ND
6	10/18/95 19	MC/S	404	N	N	N	10/16-17:10 DSF	S08W08	ND
7	10/22/95 21	S	440	10/20	N	N	10/20-05:54 XCME	S09W55	ND
8	12/16/95 05	MC/S	396	N	N	N	12/15-19:44? DSF	S02W15	ND
9	05/27/96 15	MC/S	370	N	N	N	05/22,23? DSF	-	DG
10	07/01/96 17	MC/S	355	N	N	N	-	-	DG
11	08/07/96 13	MC/S	344	N	N	N	08/05-07:50 DSF	S07W38	DG
12	12/24/96 03	MC/S	355	N	N	N	12/19-16:30 HCME	S13W10	332
13	01/10/97 05	MC/S	436	N	N	Y	01/06-15:10 HCME	S18E06	211
14	02/10/97 03	MC/S	470	N	N	N	02/07-00:30 DSF,HCME	S20W45	804
15	04/11/97 05	E/S	460	04/07	Y	N	04/07-14:27 DSF,HCME	S30E19	830
16	04/21/97 15	MC/S	360	N	N	N	04/16-07:35 DSF,HCME	S22E04	247
17	05/15/97 09	MC/S	450	05/12	Y	Y	05/12-06:30 DSF,HCME	N23W07	306
18	06/08/97 22	MC/S	370	N	N	N	06/05-22:55 DSF,CME	S35W17	417
19	06/19/97 06	E/S	350	N	N	N	06/15-12:27 DSF	N17W12	-
20	07/15/97 06	MC/S	360	N	N	N	07/11-01:30 CME?	?	-
21	08/03/97 14	MC/S	445	N	N	N	07/30-19:32 DSF,CME	N45E21	530
22	09/03/97 07	E/S	410	N	N	Y	08/30-01:30 DSF,HCME	N30E17	427
23	09/18/97 00	MC/S	320	N	N	N	09/13-11:33 CME?	N28E60	418
24	09/21/97 22	MC/S	425	09/17	N	Y	09/17-20:28 DSF,HCME	N30W10	487
25	10/01/97 16	MC/S	450	*09/26,28	N	N	09/28-01:08 DSF,HCME	N22E05	355
26	10/10/97 23	MC/S	396	*10/07,09	N	Y	10/06-15:28 DSF,HCME	S54E46	523
27	11/07/97 22	MC/S	415	*(6) 11/3,4	Y	Y	11/04-06:10 HCME	S14W33	830
28	11/09/97 10	S	400	11/6	Y	N	11/06-12:10 CME	S18W63	1560
29	11/22/97 14	E/S	490	N	N	Y	11/19-12:27 HCME	-	206
30	11/30/97 07	S	450	11/27	Y	N	11/27-13:56 CME	N16E63	434
31	12/10/97 19	E	400	N	N	N	12/06 10:27 DSF,HCME	N47W13	665
32	12/30/97 08	E/S	350	N	N	N	12/26-02:31 DSF,HCME	S24E14?	347
33	01/07/98 03	MC/S	375	N	N	N	01/02-23:28 DSF,HCME	N47W03	446
34	01/08/98 14	MC/S	355	N	N	N	01/03-09:42 DSF,CME?	-	978
35	01/24/98 04	S	400	*01/19	Y	Y	01/21-06:37 DSF,HCME	S57E19	374
36	01/28/98 15	S	410	*01/25,26	Y	Y	01/25-15:26 DSF,HCME	N24E27	562
37	01/31/98 15	S	450	*01/26,27	N	N	01/28-14:56 CME	W90	408
38	02/04/98 04	MC/S	320	N	N	N	02/02? DSF	N29E15	-
39	02/18/98 08	S/E	440	N	N	N	02/14 07:00 DSF,HCME	-	275
40	03/04/98 14	MC/S	360	N	N	Y	02/28-12:48 HCME	S24W01	155
41	04/23/98 17	S	400	04/20	Y	Y	04/20-10:07 HCME	S43W90	1638
42	04/30/98 08	S	390	04/27	Y	Y	04/27-08:56 HCME	S16E50	1631
43	05/02/98 12	MC	515	4/29	N	Y	04/29-16:58 HCME	S18E20	1016
44	05/04/98 12	E/S	650	04/29,05/01	Y	Y	05/02-14:06 HCME	S15W15	1044
45	05/15/98 13	S	350	*05/14	Y	Y	05/11-21:55 HCME	W90	877
46	05/29/98 15	S	670	N	Y	N	05/27-13:45 HCME	N19W66	957
47	06/13/98 19	S	390	06/11	Y	Y	06/11-10:28 HCME	E90	1312
48	06/24/98 12	MC	463	*06/20,22	Y	N	06/21-05:35 HCME	N16W38	307
49	06/25/98 16	S	460	*06/20,22	Y	N	06/21-18:16 CME	W90	822

DSF = dissapearing filament; CME = coronal mass ejection; HCME = halo CME; XCME - from X-ray observations.
*see text

Table 3. List of DH Type II Bursts

SNo	Date/time	Type II		CME			Flare			IP
		Metric	km	Time *	Speed	Width	Loc.	Onset	Imp.	Event
1	970401 14:00	Y	N	15:18	296	67	S25E16	13:43	M	-
2	970407 14:30	Y	Y	14:27	830	halo	S30E19	13:50	C	S/MC
3	970512 05:15	Y	Y	06:30	273	halo	N21W08	04:42	C	S/MC
4	970923 21:53	N	N	22:02	760	170	S29E30	21:27	C	-
5	971103 05:15	Y	Y	05:28	369	90	S20W13	04:32	C	-
6	971103 10:30	Y	N	11:11	420	195	S20W15	10:18	M	-
7	971104 06:00	Y	Y	06:10	830	halo	S14W33	05:52	X	S/MC
8	971106 12:20	Y	Y	12:10	1561	155	S18W63	11:49	X	S
9	971127 13:30	Y	N	13:56	434	82	N16E63	12:59	X	S
10	971212 22:45	N	N	00:26 $^{+}$	166	64	N25W52	22:05	B	-
11	980121 10:40	N	Y	06:37	296	halo	S57E19	07:34	B	S
12	980125 15:12	N	Y	15:26	481	halo	N24E27	14:29	C	S
13	980329 03:15	Y	N	03:48	1361	halo	back	02:44	O	-
14	980420 10:25	Y	Y	10:07	1631	264	S43W90	09:38	M	S
15	980423 06:00	Y	Y	04:20	1222	halo	S19E90	05:35	X	-
16	980427 09:25	Y	Y	08:56	1221	halo	S16E50	08:55	X	S
17	980502 14:10	N	N	14:06	1039	halo	S15W15	13:31	X	S/E
18	980503 22:30	N	N	22:02	705	240	S13W34	21:15	M	-
19	980506 08:25	Y	N	08:29	1053	185	S11W65	07:10	M	-
20	980509 03:35	Y	Y	03:35	1763	143	S11W90	03:04	M	-
21	980511 21:40	N	Y	21:55	611	270	N29W90	21:28	O	S
22	980519 10:00	Y	N	10:27	672	115	N29W46	09:26	-	-
23	980527 13:30	N	N	13:45	677	238	N19W66	13:18	C	S
24	980611 10:15	Y	Y	10:28	1159	156	S21E80	09:57	M	S
25	980616 18:20	Y	Y	18:27	1245	252	S17W90	18:03	M	-
26	980620 21:10	N	N	18:20	1038	halo	back	20:54	C	-
27	980622 07:15	N	N	18:15$^{@}$	822	94	N37W80	-	-	S

O = occulted event; S = shock; MC = magnetic cloud; E = ejecta
*UT time corresponding to first sighting in C2 Coronagraph.
$^{+}$next day.
$^{@}$previous day.

:

:

:

:

:

:

:

: